

Stereostructure of a Novel Cytotoxic 18-Membered Macrolactone Antibiotic FD-891

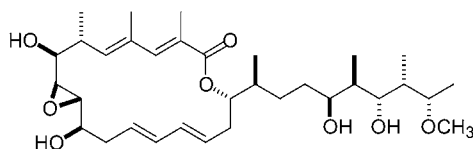
Tadashi Eguchi,^{*,†} Kayako Kobayashi,[†] Hidehiro Uekusa,[†] Yuji Ohashi,[†]
Kazutoshi Mizoue,[‡] Yoshitaka Matsushima,[§] and Katsumi Kakinuma^{*,§}

Department of Chemistry and Materials Science, Tokyo Institute of Technology,
O-okayama, Meguro-ku, Tokyo 152-8551, Japan, Research Laboratories, Taisho
Pharmaceutical Co., Ltd., 1-403, Yoshino-cho, Saitama-shi, Saitama 330-8530, Japan,
and Department of Chemistry, Tokyo Institute of Technology, O-okayama, Meguro-ku,
Tokyo 152-8551, Japan

eguchi@cms.titech.ac.jp

Received July 14, 2002

ABSTRACT



FD-891

The absolute stereochemistry of FD-891, a novel cytotoxic 18-membered macrolactone antibiotic, was determined by a synthetic approach as well as X-ray diffraction of degradative derivatives. The absolute configuration of FD-891 turned out to be as shown above. The stable conformer of FD-891 was also discussed with respect to biological activity by comparison with the structurally related concanamycin A on the bases of molecular mechanics calculations.

FD-891 (**1**) was isolated from the fermentation broth of *Streptomyces graminofaciens* A-8890 and was shown to have cytotoxic activity in vitro against several tumor cell lines.¹ The planar structure of **1** was elucidated to be an 18-membered macrolactone by spectroscopic means as shown in Figure 1,² which appeared to be related to a specific inhibitor of vacuolar-type H⁺-ATPase, concanamycin A.³ In recent years, concanamycin A has been shown to specifically inhibit perforin-dependent cytotoxic T lymphocyte (CTL)-mediated cytotoxicity but not affect Fas ligand

[†] Department of Chemistry and Materials Science, Tokyo Institute of Technology.

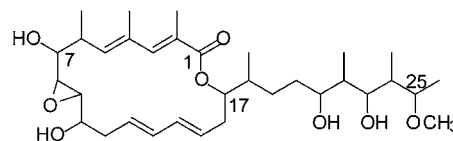
[‡] Taisho Pharmaceutical Co., Ltd.

[§] Department of Chemistry, Tokyo Institute of Technology.

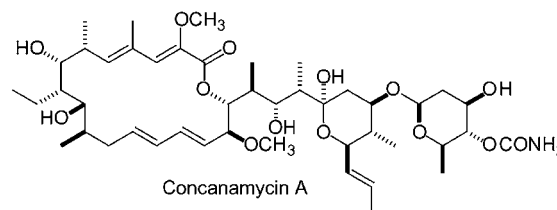
(1) Seki-Asano, M.; Okazaki, T.; Yamagishi, M.; Sakai, N.; Hanada, K.; Mizoue, K. *J. Antibiot.* **1994**, *47*, 1226.

(2) Seki-Asano, M.; Tsuchida, Y.; Hanada, K.; Mizoue, K. *J. Antibiot.* **1994**, *47*, 1234.

(3) (a) Muroi, M.; Shiragami, N.; Nagao, K.; Yamasaki, M.; Takatsuki, A. *Cell Struct. Funct.* **1993**, *18*, 139. (b) Drose, S.; Bindseil, K. U.; Bowman, E. J.; Siebers, A.; Zeeck, A.; Altendorf, K. *Biochemistry* **1993**, *32*, 3902.



FD-891 (**1**)

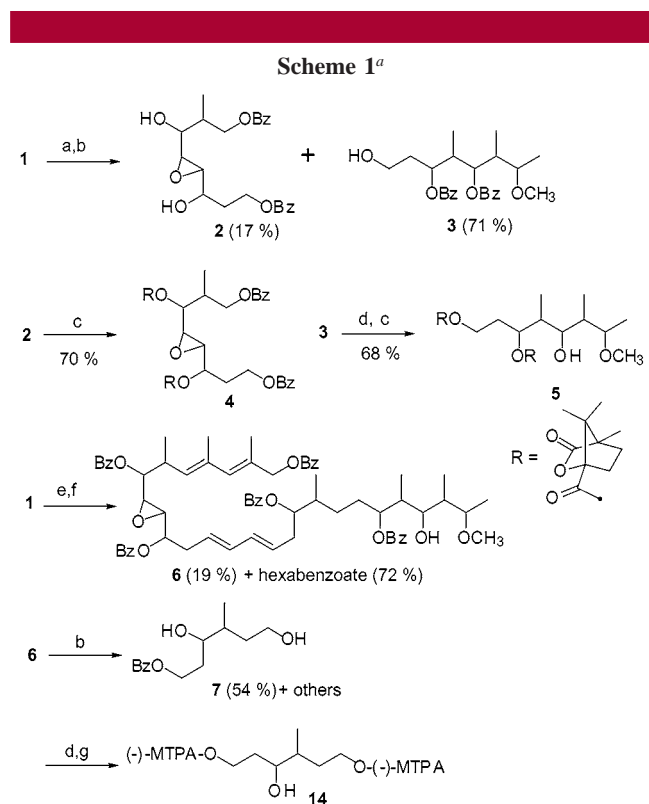


Concanamycin A

Figure 1. Structures of FD-891 (**1**) and concanamycin A.

(FasL)-dependent CTL-mediated cytotoxicity. These two cytotoxic pathways play an essential role in the maintenance of tissue homeostasis.⁴ In contrast, **1** was found to potently prevent both perforin- and FasL-dependent CTL-mediated killing pathways. Moreover, **1** was, in contrast to concanamycin A, unable to inhibit vacuolar acidification.⁵ These specific biological features of **1** prompted us to study the chemical basis of its activity in relation to concanamycin A and related cytotoxic macrolactone compounds. However, since the stereochemistry of **1** has not been elucidated to date, we first pursued chemical studies to elucidate the absolute stereochemistry as well as the stable conformation of **1**.

Since NMR analysis, including various NOE experiments, was not informative for the configurational analysis of **1** and modification into a crystalline derivative was not successful either, we undertook degradation studies of **1**. First, **1** was benzoylated in a conventional way to the corresponding tetrabenzoate in high yield, which was then subjected to ozonolysis. After reductive workup with NaBH₄ of the resulting ozonides, two fragments were isolated and found to be the C₅–C₁₂ fragment **2** and the C₁₉–C₂₆ fragment **3** by spectroscopic analysis as shown in Scheme 1.⁶ Interest-



^a Reaction conditions: (a) BzCl, DMAP/py; (b) O₃/MeOH, and then NaBH₄; (c) (–)-camphanic chloride, DMAP/py; (d) MeOK–MeOH; (e) DIBAL/CH₂Cl₂; (f) BzCl/py; (g) (R)-(-)-MTPACl, DMAP/py.

ingly, both benzoyl groups were migrated from secondary hydroxy groups to primary ones in the fragment **2**. Unexpectedly further, the fragment **3** appeared to be the product by unusual oxidative cleavage of the C₁₈–C₁₉ bond under

these conditions. The reason such an unusual oxidative cleavage occurred is not clear. Moreover, a fragment comprised of C₁₅–C₂₆ was not obtained at all under several reaction conditions.

For the unambiguous assignment of the absolute stereochemistry of these fragments, we attempted chemical transformation of **2** and **3** into crystalline derivatives for X-ray analysis. Fortunately, the dicamphanic ester derivative **4**, which was obtained by treatment of **2** with (–)-camphanic chloride in pyridine in the presence of 4-(dimethylamino)pyridine, formed suitable crystals for X-ray analysis by recrystallization from hexanes–ethyl acetate. The absolute stereochemistry of the C₆–C₁₀ of **1** was clearly determined as shown in Figure 2 simply on the basis of the absolute

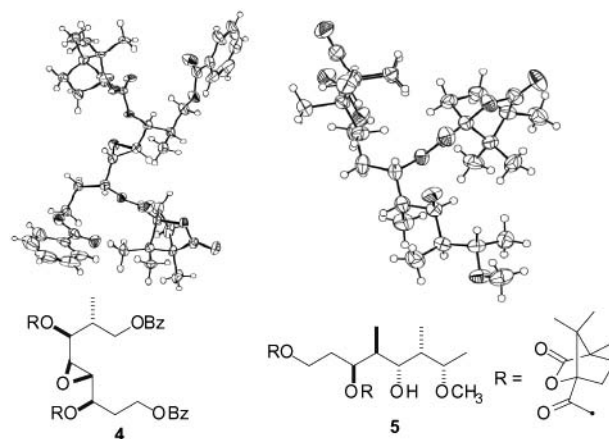


Figure 2. ORTEP drawings of **4** and **5** (thermal ellipsoids at the 25% probability level) and the absolute stereostructures of **4** and **5**.

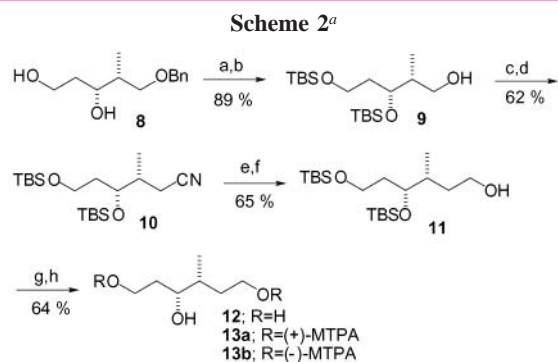
structure of (–)-camphanic ester structure. As to the fragment **3**, hydrolysis with MeOK–MeOH, followed by esterification similarly with (–)-camphanic chloride gave crystalline derivative **5** by recrystallization again from hexanes–ethyl acetate. Thus, the absolute stereochemistry of the C₂₁–C₂₅ portion of **1** was also determined by X-ray crystallography as shown in Figure 2.

At this stage, the remaining stereogenic centers to be determined were C₁₇ and C₁₈. Because a fragment containing C₁₇ and C₁₈ was not available from ozonolysis of the tetrabenzoate derivative as described above, we modified a substrate of ozonolysis. Thus, **1** was first subjected to reduction with DIBAL, followed by benzoylation with benzoyl chloride in pyridine, to give pentabenzoate **6** and the corresponding hexabenzoate. The minor product **6** turned out to be crucial. A fragment **7** containing C₁₇ and C₁₈ stereogenic centers was obtained in 54% yield as an unusual oxidative cleavage and benzoyl migrated product, only when

(4) Kataoka, T.; Shinohara, N.; Takayama, H.; Takaku, K.; Kondo, S.; Yonehara, S.; Nagai, K. *J. Immunol.* **1996**, *156*, 3678.

(5) Kataoka, T.; Yamada, A.; Bando, M.; Honma, T.; Mizoue, K. Nagai, K. *Immunology* **2000**, *100*, 170.

6 was used as a substrate of ozonolysis (Scheme 1).⁶ The reason is not clear again. Since the fragment **7** included only two stereogenic centers, we took advantage of the chemical synthesis of the fragment **7** in a stereochemically defined manner. The relative stereochemistry of the fragment **7** was envisioned to be syn (*S,S* or *R,R*), because the ¹H–¹H coupling constant between two stereogenic centers of **7** was relatively small (*J* = 3.2 Hz). Consequently, we synthesized the authentic sample from the known (*R,R*)-diol **8**⁷ as shown in Scheme 2. Protection of hydroxy groups of **8** with a TBS



^a Reaction conditions: (a) TBSCl, imidazole/DMF; (b) H₂, Pd–C/EtOH; (c) MsCl, Et₃N/CH₂Cl₂; (d) NaCN/DMSO; (e) DIBAL/toluene; (f) NaBH₄/MeOH; (g) 2 N HCl/THF; (h) (*S*)-(+)-MTPACl, DMAP/py or (*R*)-(–)-MTPACl, DMAP/py.

group and deprotection of the benzyl group by hydrogenation afforded **9** in high yield. The primary hydroxy group of **9** was displaced with a cyano group via its mesylate to give **10**. Reduction of **10** with DIBAL, followed further by NaBH₄ reduction, gave alcohol **11** in 65% yield. Acidic hydrolysis of **11** with 2 N HCl yielded triol **12**.

The triol **12** was converted into di-(+)- or (–)-MTPA esters **13a** or **13b**, respectively, in order to be compared with the corresponding naturally derived MTPA ester. Thus, the above-mentioned fragment **7** was hydrolyzed with MeOK–MeOH, and the resulting triol was then treated with

(6) Spectroscopic data of compounds **2**, **3**, and **7**. **Compound 2**: ¹H NMR (500 MHz, CDCl₃) δ 1.07 (d, *J* = 7.3 Hz, 3H), 1.98–2.12 (m, 2H), 2.21–2.26 (m, 1H), 3.14 (dd, *J* = 2.3, 3.2 Hz, 1H), 3.23 (dd, *J* = 2.3, 4.2 Hz, 1H), 3.81 (m, 1H), 3.98 (m, 1H), 4.26 (dd, *J* = 5.9, 11.1 Hz, 1H), 4.44 (dd, *J* = 8.0, 11.0 Hz, 1H), 4.51 (dt, *J* = 11.3, 5.7 Hz, 1H), 4.56 (ddd, *J* = 5.3, 8.4, 11.2 Hz, 1H), 7.42 (m, 4H), 7.56 (m, 2H), 8.02 (m, 4H); ¹³C NMR (126 MHz, CDCl₃) δ 10.9, 33.8, 35.9, 57.1, 58.0, 61.3, 66.4, 67.2, 68.3, 128.4, 128.5, 129.6, 129.6, 130.0, 133.1, 133.1, 166.7, 166.7. **Compound 3**: ¹H NMR (500 MHz, CDCl₃) δ 1.04 (d, *J* = 7.0 Hz, 3H), 1.15 (d, *J* = 6.2 Hz, 3H), 1.19 (d, *J* = 7.1 Hz, 3H), 1.80–1.81 (m, 1H), 1.93–2.00 (m, 1H), 2.01–2.04 (m, 1H), 2.26 (double quintet, *J* = 2.0, 7.1 Hz, 1H), 3.19 (s, 3H), 3.24 (dq, *J* = 6.1, 6.2 Hz, 1H), 3.49 (m, 1H), 3.65 (m, 1H), 5.33 (dd, *J* = 4.1, 7.6 Hz, 1H), 5.52 (dt, *J* = 9.7, 2.3 Hz, 1H), 7.26 (dd, *J* = 7.7, 7.8 Hz, 2H), 7.36 (t, *J* = 7.7 Hz, 2H), 7.44 (t, *J* = 7.3 Hz, 1H), 7.51 (dd, *J* = 8.3, 1.2 Hz, 1H), 7.86 (dd, *J* = 8.3, 1.2 Hz, 2H), 7.94 (d, *J* = 8.2 Hz, 2H); ¹³C NMR (126 MHz, CDCl₃) δ 9.7, 11.4, 16.2, 36.0, 39.0, 40.2, 56.4, 58.4, 69.9, 76.1, 79.0, 128.1, 128.3, 129.5, 129.6, 130.2, 130.3, 132.6, 132.9, 166.1, 167.3. **Compound 7**: ¹H NMR (500 MHz, CDCl₃) δ 0.95 (d, *J* = 6.9 Hz, 3H), 1.55 (ddt, *J* = 4.7, 14.3, 6.4 Hz, 1H), 1.74 (ddt, *J* = 6.2, 14.5, 7.2 Hz, 1H), 1.84 (double sextet, *J* = 3.2, 6.8 Hz, 1H), 1.90 (m, 2H), 3.67 (ddd, *J* = 4.6, 7.6, 10.9 Hz, 1H), 3.76 (m, 2H), 4.44 (ddd, *J* = 5.6, 5.6, 11.2 Hz, 1H), 4.61 (dt, *J* = 11.3, 6.8 Hz, 1H), 7.45 (t, *J* = 7.8 Hz, 2H), 7.57 (m, 1H), 8.04 (m, 2H); ¹³C NMR (126 MHz, CDCl₃) δ 14.4, 32.8, 36.0, 36.4, 60.7, 62.7, 71.4, 128.4, 129.6, 133.0, 167.1.

(*R*)-(–)-MTPA chloride to give di-(–)-MTPA ester **14**. The ¹H NMR spectrum of naturally derived (–)-MTPA ester **14** was quite different from that of the synthetic (–)-MTPA ester **13b** but completely identical to that of (+)-MTPA ester **13a** as shown in Figure 3. Consequently, the absolute stereo-

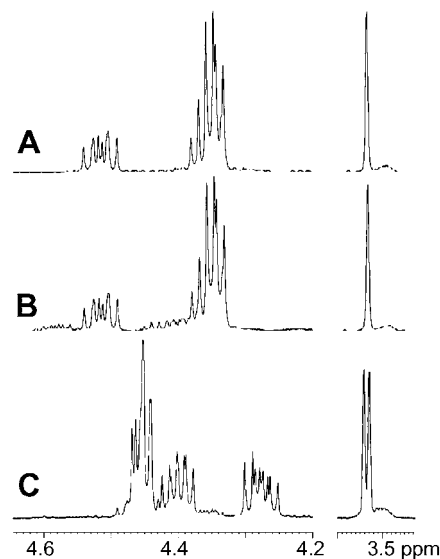


Figure 3. Partial ¹H NMR spectra (500 MHz, CDCl₃) of (A) (+)-MTPA ester **13a**, (B) naturally derived (–)-MTPA ester **14**, and (C) (–)-MTPA ester **13b**.

chemistry of C₁₇–C₁₈ of **1** was proven to be enantiomeric to the synthetic triol **12**. In conclusion, by combining all the data discussed above, the absolute stereochemistry of **1** was unequivocally determined as shown in Figure 4.

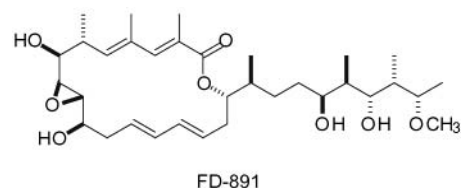


Figure 4. Absolute stereochemistry of FD-891 (**1**).

As described above, FD-891 (**1**) appeared to be structurally related to concanamycin A. However, the biological characteristics of these two natural products are fairly different. These findings raised a question of how **1** and concanamycin A exert their effect at the molecular level. As the first step, we initiated detailed conformational and structure–activity investigations of **1** and concanamycin A. Molecular modeling approach has been frequently used to determine the lower

(7) (a) Arai, H.; Matsushima, Y.; Eguchi, T.; Shindo, K.; Kakinuma, K. *Tetrahedron Lett.* **1998**, 39, 3181. (b) Ireland, R. E.; Thaisrivongs, S.; Dussault, P. H. *J. Am. Chem. Soc.* **1988**, 110, 5768.

energy conformations of a molecule of interest. We took advantage of recent advances in molecular modeling techniques to carry out conformational analysis of **1** and concanamycin A.⁸ The calculated most stable conformation of **1** is shown in Figure 5.

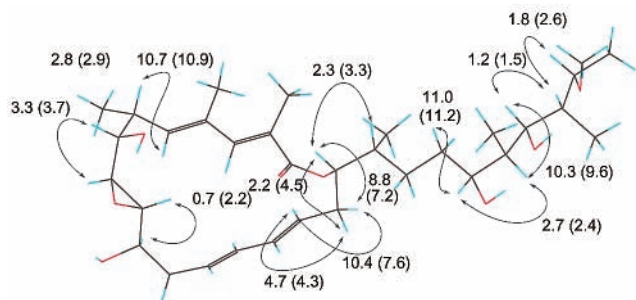


Figure 5. Most stable conformation of FD-891. Values are the calculated ^1H – ^1H coupling constants (in hertz) deduced from the Karplus–Altona equation with Boltzmann averaging.¹³ Experimentally observed data are given in parentheses.

The Boltzmann averaged ^1H – ^1H coupling constants deduced from the Karplus–Altona equation¹³ are also summarized in Figure 5. These values are in good accordance with the observed coupling constants, which supports well the reliability of these calculations. As to concanamycin A, the most stable conformation is quite similar to the crystalline state structure.¹⁴ These results secure the conformational

(8) A conformational search and energy minimization of FD-891 and concanamycin A were performed using the MMFF force field⁹ in MacroModel version 6.5.¹⁰ All calculations were performed using the implicit CHCl_3 GB/SA solvation model of Still et al.¹¹ A conformational search was performed using the Monte Carlo method of Goodman and Still.¹² For each search, 20 000 starting structures were generated and minimized to an energy convergence of 0.05 (kJ/mol)/(Å/mol) using the full matrix Newton–Raphson method implemented in MacroModel. Duplicated structures and those greater than 50 kJ/mol above the global minimum were discarded.

(9) (a) Halgren, T. A. *J. Comput. Chem.* **1996**, *17*, 490. (b) Halgren, T. A. *J. Comput. Chem.* **1996**, *17*, 520. (c) Halgren, T. A. *J. Comput. Chem.* **1996**, *17*, 553. (d) Halgren, T. A. *J. Comput. Chem.* **1996**, *17*, 587.

(10) *MacroModel Version 6.5*; Department of Chemistry, Columbia University: New York.

(11) (a) Hasel, W.; Hendrickson, T. F.; Still, W. C. *Tetrahedron Comput. Methodol.* **1988**, *1*, 103. (b) Still, W. C.; Tempczyk, A.; Hawley, R. C.; Hendrickson, T. *J. Am. Chem. Soc.* **1990**, *112*, 6127.

(12) (a) Chang, G.; Guida, W. C.; Still, W. C. *J. Am. Chem. Soc.* **1989**, *111*, 5239. (b) Goodman, J. M.; Still, W. C. *J. Comput. Chem.* **1991**, *12*, 1110. (c) Guida, W. C.; Bohacek, R. S.; Erion, M. D. *J. Comput. Chem.* **1992**, *13*, 214. (d) Kolossvary, I.; Guida, W. C. *J. Chem. Inf. Comput. Sci.* **1992**, *32*, 191. (e) Kolossvary, I.; Guida, W. C. *J. Comput. Chem.* **1993**, *14*, 691. (f) Kolossvary, I.; Guida, W. C. *J. Am. Chem. Soc.* **1993**, *115*, 2107.

(13) Haasnoot, C. A. G.; De Leeuw, F. A. M.; Altona, C. *Tetrahedron* **1980**, *36*, 2783.

(14) Nakai, H.; Matsuhashi, S. *Acta Crystallogr.* **1992**, *C48*, 1519.

arguments of these two compounds. An interesting feature found in the structure of concanamycin A was a hydrogen-bond network through lactone carbonyl/19-hydroxy group/six-membered hemiketal hydroxy group, which could restrict the side chain conformation. The structure–activity relationship studies of concanamycins previously revealed that the 18-membered lactone ring conformation and the hydrogen-bond network were crucial for the inhibitory effects on vacuolar-type H^+ –ATPase activity as well as lysosomal acidification, but the carbohydrate residue was dispensable for these activities.^{3b,15}

As can be seen in the superimposed structures of **1** and concanamycin A (Figure 6), although the hydrogen bond

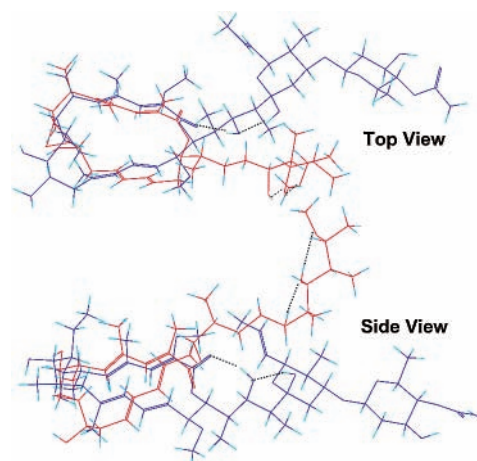


Figure 6. Superimposed view of FD-891 and concanamycin A. (Red) FD-891, (blue) concanamycin A. Dashed lines indicate a hydrogen-bond network.

network exists in the most stable conformation of **1**, the conformation of macrolactone ring and the direction of the side-chain are quite different from each other. It appears therefore that, although the major chemical difference between FD-891 and concanamycin A is obviously found in their side-chain structure, the macrolactone conformation is also significantly different, which may well affect their biological activity. Further structure–activity relationship study of this class of antibiotics is underway.

Supporting Information Available: Experimental procedure of compounds **2**–**12** and X-ray crystallographic data of **4** and **5**. This material is available free of charge via the Internet at <http://pubs.acs.org>.

OL026518K

(15) (a) Droese, S.; Boddien, C.; Gassel, M.; Ingenhorst, G.; Zeeck, A.; Altendorf, K. *Biochemistry* **2001**, *40*, 2816. (b) Woo, J. T.; Shinohara, C.; Sakai, K.; Hasumi, K.; Endo, A. *J. Antibiot.* **1992**, *45*, 1108.